Angiogenesis (2021) 24:97–110
https://doi.org/10.1007/s10456-020-09745-7

ORIGINAL PAPER

A drug-tunable Flt23k gene therapy for controlled intervention in retinal neovascularization

Jinying Chen[1,2] · Fan-Li Lin[2,3] · Jacqueline Y. K. Leung[4] · Leilei Tu[1] · Jiang-Hui Wang[5] · Yu-Fan Chuang[2,4] · Fan Li[2,6] · Hsin-Hui Shen[7,8] · Gregory J. Dusting[5,9] · Vickie H. Y. Wong[10] · Leszek Lisowski[11,12,13] · Alex W. Hewitt[2,5,9] · Bang V. Bui[10] · Jingxiang Zhong[1] · Guei-Sheung Liu[1,2,9]

Received: 3 February 2020 / Accepted: 4 September 2020 / Published online: 15 September 2020

Abstract

Gene therapies that chronically suppress vascular endothelial growth factor (VEGF) represent a new approach for managing retinal vascular leakage and neovascularization. However, constitutive suppression of VEGF in the eye may have deleterious side effects. Here, we developed a novel strategy to introduce Flt23k, a decoy receptor that binds intracellular VEGF, fused to the destabilizing domain (DD) of *Escherichia coli* dihydrofolate reductase (DHFR) into the retina. The expressed DHFR(DD)-Flt23k fusion protein is degraded unless "switched on" by administering a stabilizer; in this case, the antibiotic trimethoprim (TMP). Cells transfected with the DHFR(DD)-Flt23k construct expressed the fusion protein at levels correlated with the TMP dose. Stabilization of the DHFR(DD)-Flt23k fusion protein by TMP was able to inhibit intracellular VEGF in hypoxic cells. Intravitreal injection of self-complementary adeno-associated viral vector (scAAV)-DHFR(DD)-Flt23k and subsequent administration of TMP resulted in tunable suppression of ischemia-induced retinal neovascularization in a rat model of oxygen-induced retinopathy (OIR). Hence, our study suggests a promising novel approach for the treatment of retinal neovascularization.

Jingxiang Zhong and Guei-Sheung Liu contributed equally to this work as senior author.

Electronic supplementary material The online version of this article (https://doi.org/10.1007/s10456-020-09745-7) contains supplementary material, which is available to authorized users.

✉ Guei-Sheung Liu
rickliu0817@gmail.com

1 Department of Ophthalmology, The First Affiliated Hospital of Jinan University, Guangzhou, Guangdong, China

2 Menzies Institute for Medical Research, University of Tasmania, Hobart, TAS, Australia

3 Shenzhen Key Laboratory of Biomimetic Materials and Cellular Immunomodulation, Shenzhen Institute of Advanced Technology, Chinese Academy of Sciences, Shenzhen, Guangdong, China

4 Wicking Dementia Research and Education Centre, University of Tasmania, Hobart, TAS, Australia

5 Centre for Eye Research Australia, Royal Victorian Eye and Ear Hospital, East Melbourne, VIC, Australia

6 State Key Laboratory of Ophthalmology, Zhongshan Ophthalmic Centre, Sun Yat-sen University, Guangzhou, Guangdong, China

7 Department of Materials Science and Engineering, Faculty of Engineering, Monash University, Clayton, VIC, Australia

8 Department of Biochemistry and Molecular Biology, School of Biomedical Science, Monash University, Clayton, VIC, Australia

9 Ophthalmology, Department of Surgery, University of Melbourne, East Melbourne, VIC, Australia

10 Department of Optometry and Vision Sciences, University of Melbourne, Parkville, VIC, Australia

11 Translational Vectorology Group, Children's Medical Research Institute, Faculty of Medicine and Health, University of Sydney, Sydney, NSW, Australia

12 Vector and Genome Engineering Facility, Children's Medical Research Institute, Faculty of Medicine and Health, University of Sydney, Sydney, NSW, Australia

13 Military Institute of Hygiene and Epidemiology, The Biological Threats Identification and Countermeasure Centre, Puławy, Poland

Graphic abstract

Schematic diagram of the tunable system utilizing the DHFR(DD)-Flt23k approach to reduce VEGF secretion. **a** The schematic shows normal VEGF secretion. **b** Without the ligand TMP, the DHFR(DD)-Flt23k protein is destabilized and degraded by the proteasome. **c** In the presence of the ligand TMP, DHFR(DD)-Flt23k is stabilized and sequestered in the ER, thereby conditionally inhibiting VEGF. Green lines indicate the intracellular and extracellular distributions of VEGF. Blue lines indicate proteasomal degradation of the DHFR(DD)-Flt23k protein. Orange lines indicate the uptake of cell-permeable TMP. TMP, trimethoprim; VEGF, vascular endothelial growth factor; ER, endoplasmic reticulum.

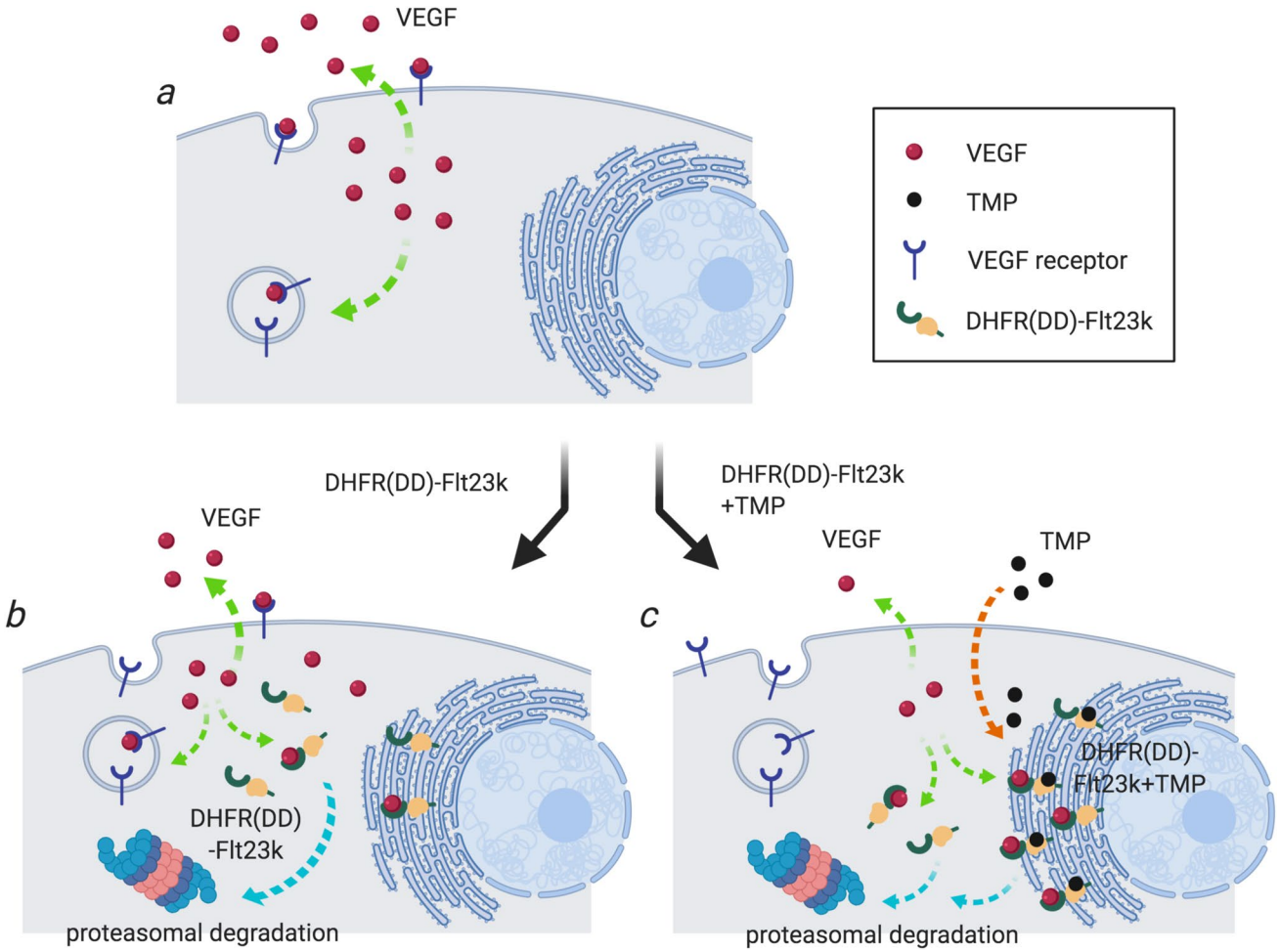

Keywords Retinal neovascularization · VEGF · Flt23k · Destabilizing domain · Trimethoprim · AAV · Gene therapy

Introduction

Retinal neovascularization is a key pathological feature of several leading causes of vision loss, including diabetic retinopathy, retinopathy of prematurity, and retinal vein occlusions [1]. In these diseases, abnormally high levels of vascular endothelial growth factor (VEGF) have been observed in the retina. Excessively high levels of VEGF cause pathological vascular leakage and the formation of new blood vessels in the retina, which can lead to vision loss. Intraocular injections of anti-VEGF agents (such as VEGF-neutralizing proteins) have been shown to reduce blood vessel leakage, allowing fluid reabsorption and resulting in improved visual acuity [2]. However, as this approach does not address the cause of VEGF production, leakage and neovascularization will recur when the vitreous levels of exogenous anti-VEGF proteins drop below therapeutic levels. Thus, current regimens require frequent (as often as monthly) and prolonged treatment, sometimes for many years, to maintain visual acuity [3]. Although intraocular delivery of anti-VEGF agents is generally safe, some of the drugs administered can enter the systemic circulation, where

chronically high levels of anti-VEGF proteins can increase the risk of systemic adverse effects [4].

Recently, the utilization of gene therapies with the potential to chronically suppress the production of VEGF in the retina has been proposed as an attractive way to manage ocular neovascularization [5, 6]. While promising, chronic VEGF suppression may have deleterious side effects on the retina. As the disease course can fluctuate between periods of relative VEGF inactivity and high activity in many patients, a gene therapy approach that can accommodate such fluctuations during the course of disease would potentially be a safer and more effective approach than an approach with prolonged VEGF suppression. In this study, we created a fusion gene consisting of an intracellular VEGF-targeting decoy receptor, Flt23k [7], and a protein disruption system (based on the destabilizing domain (DD) of *Escherichia coli* dihydrofolate reductase (DHFR); DHFR (DD)-Flt23k) [8, 9]. Flt23k consists of domains 2–3 of VEGF receptor 1 (VEGFR1, the highest-affinity VEGF receptor) coupled to the C-terminal endoplasmic reticulum (ER) retention signal KDEL, a tetrapeptide (Lys-Asp-Glu-Leu). Flt23k binds intracellular VEGF and sequesters it in the ER, where VEGF undergoes proteasomal degradation [10, 11]. Without a triggering molecule, the expressed DHFR(DD)-Flt23k fusion protein becomes unfolded and ubiquitinated and then is rapidly processed by the proteasome, resulting in degradation of the entire fusion protein [12]. A stabilizing drug such as the antibiotic trimethoprim (TMP) reliably prevents proteasomal destruction of DHFR(DD)-Flt23k, which then binds to intracellular VEGF and prevents VEGF secretion (Fig. 1a, illustration). In addition, to achieve long-term and early-onset gene expression, a self-complementary adeno-associated viral vector (scAAV) [13] was utilized to deliver the *DHFR(DD)-Flt23k* gene into the back of the eye via a single intravitreal injection. Our data demonstrated that gene delivery of *DHFR(DD)-Flt23k* and subsequent administration of TMP allowed disruption of VEGF levels in vitro. Importantly, we also showed that this approach resulted in tunable suppression of retinal neovascularization in a rat model of oxygen-induced retinopathy (OIR).

Results

Design and validation of the DHFR-based destabilized domain approach in vitro

scAAVs encoding enhanced green fluorescent protein (EGFP) (or mCherry), Flt23k, DHFR(DD)-yellow fluorescent protein (YFP) (or DHFR(DD)-mCherry), DHFR(DD)-Flt23k, or Flt23k-DHFR(DD) were designed and constructed for the study (Fig. 1b). We first validated whether the DHFR(DD)-protein-destabilizing system could be controlled using the stabilizing ligand TMP in vitro. Human embryonic kidney 293A (HEK293A) cells were transfected with scAAV plasmid (pscAAV)-mCherry, pscAAV-Flt23k, pscAAV-DHFR(DD)-YFP, pscAAV-DHFR(DD)-Flt23k or pscAAV-Flt23k-DHFR(DD) for 24 h and then exposed to 10 μM TMP or varying doses of TMP (0, 2, 10, and 50 μM) for 24 h. A 42-kDa band for DHFR(DD)-Flt23k or Flt23k-DHFR(DD) or a 25-kDa Flt23k protein was detectable in pscAAV-DHFR(DD)-Flt23k, pscAAV-Flt23k-DHFR(DD) and pscAAV-Flt23k-transfected cells, respectively, by western blotting. Neither protein was found in pscAAV-DHFR(DD)-YFP- or pscAAV-mCherry-transfected cells (Fig. 1c). Compared with the construct with C-terminal fusion of Flt23k (Flt23k-DHFR(DD): 1.41-fold increase, $p < 0.05$; $n = 3$), the construct with N-terminal fusion (DHFR(DD)-Flt23k: 2.66-fold increase, $p < 0.001$; $n = 3$) was more flexibly regulated by TMP, as evidenced by relatively low DHFR(DD)-Flt23k protein levels in the absence of TMP and high levels following TMP exposure (Fig. 1d). Interestingly, we observed a slight increase in DHFR(DD)-Flt23k expression in pscAAV-DHFR(DD)-Flt23k-transfected cells even without TMP, indicating that some undegraded proteins remained despite the DHFR(DD)-protein-destabilizing system.

Next, we investigated whether DHFR(DD)-Flt23k is dependent on the TMP dose in vitro. Compared to no TMP, the addition of 2, 10 or 50 μM TMP to the culture medium resulted in an increase in cytosolic DHFR(DD)-Flt23k expression (2 μM: 2.12-fold, 10 μM: 3.14-fold, 50 μM: 4.45-fold; $p < 0.05$, $n = 4$) (Fig. 1e and f). Although DHFR(DD)-Flt23k protein levels rose with increasing doses of TMP, no significant difference was found between 10 and 50 μM TMP treatment ($p = 0.2330$). These data suggest that the N-terminal fusion construct DHFR(DD)-Flt23k is more flexibly regulated and can be dose-dependently stabilized by TMP.

Stabilization of DHFR(DD)-Flt23k functionally inhibits hypoxia-induced VEGF in vitro

Next, we considered whether the product resulting from TMP induction of DHFR(DD)-Flt23k was biologically active by examining its capacity to inhibit hypoxia-induced human VEGF production. HEK293A cells were transfected with pscAAV-DHFR(DD)-Flt23k for 24 h and exposed to TMP at a dose between 0 and 50 μM for 24 h. The cells were incubated under hypoxic conditions for 24 h. Cell lysates and conditioned medium were harvested for enzyme-linked immunosorbent assay (ELISA)-based detection of VEGF. Under the hypoxic conditions, compared to pscAAV-mCherry-transfected cells, the cells transfected with pscAAV-Flt23k (intracellular VEGF: 190 ± 27 pg/μg, $p < 0.05$, $n = 6$–7; extracellular VEGF: 1156 ± 107 pg/mL, $p < 0.05$, $n = 7$) showed reductions in both intracellular and extracellular VEGF levels (intracellular VEGF: 315 ± 32 pg/

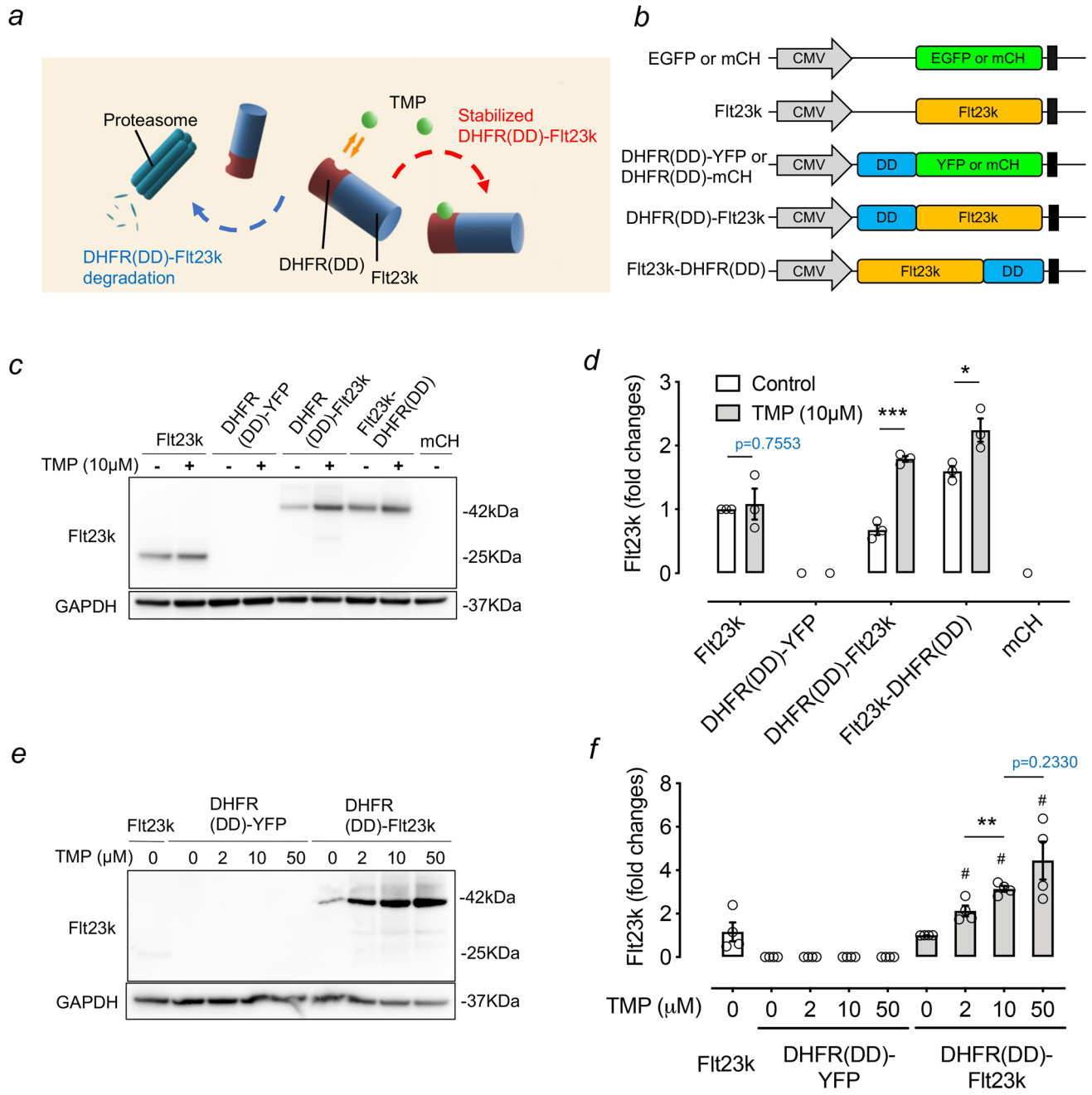

Fig. 1 Characterization of DHFR(DD)-Flt23k gene transfer in vitro. **a** The schematic illustrates conditional protein stabilization by the ligand TMP. The DHFR(DD)-fused Flt23k protein is an unstable cytosolic protein that is rapidly degraded by the proteasome unless protected by the specific cell-permeable ligand TMP. **b** The schematic shows plasmid constructs. **c** and **d** 2 days after transfection, the expression of Flt23k or DHFR(DD) fused with Flt23k in HEK293A cells in the presence of 0 or 10 µM TMP was confirmed by western blotting. The graph shows the quantification of protein expression. Two-tailed Student's *t*-tests were performed to determine the significance of differences (***$p<0.001$, *$p<0.05$). **e** and **f** The DHFR(DD)-Flt23k level in HEK293A cells was increased by TMP in a dose-dependent manner (0–50 µM). The graph shows the quantification of protein expression. Two-tailed Student's *t*-tests were performed to determine the significance of differences (**$p<0.01$; $^{\#}p<0.05$ compared to DHFR(DD)-Flt23k with 0 µM TMP). All data are presented as the mean ± SEM. Corresponding uncropped images of western blots are shown in Figure S6. CMV, cytomegalovirus; mCH, mCherry; EGFP, enhanced green fluorescent protein; YFP, yellow fluorescent protein; TMP, trimethoprim

µg; extracellular VEGF: 1564 ± 102 pg/mL; $n=5$) (Fig. 2a, b). Cells transfected with pscAAV-DHFR(DD)-Flt23k showed a significant decrease in the intracellular VEGF concentration, an effect that was dependent on the dose of TMP (DHFR(DD)-Flt23k: 198 ± 19 pg/µg; DHFR(DD)-Flt23k with 2 µM TMP: 95 ± 16 pg/µg; DHFR(DD)-Flt23k

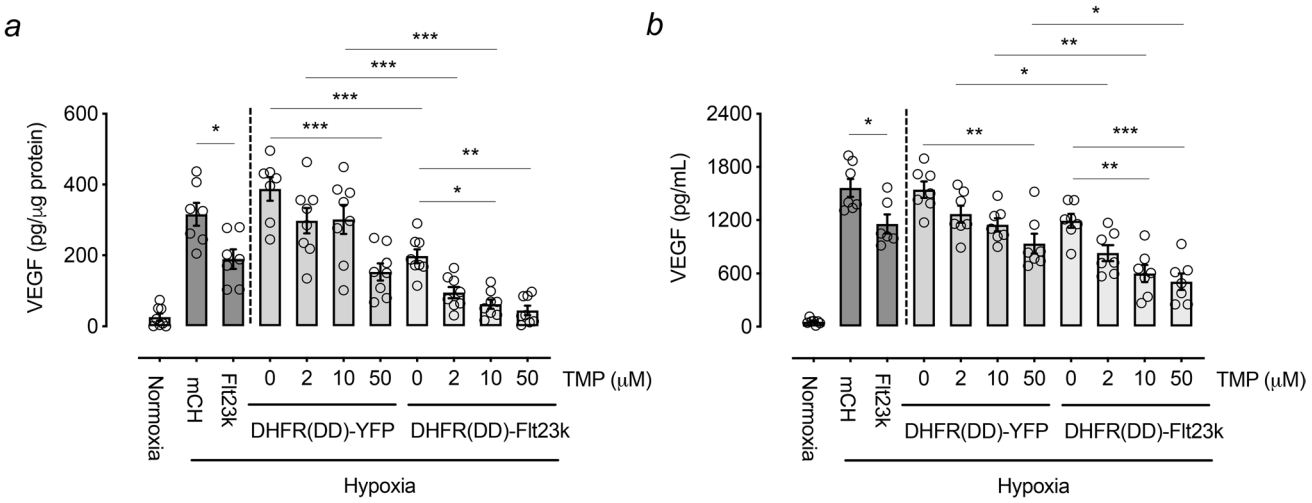

Fig. 2 Stabilization of DHFR(DD)-Flt23k inhibits intracellular and extracellular VEGF. Cells were transfected and treated with different doses of TMP (0, 2, 10, or 50 μM), followed by treatment with hypoxia for 24 h. Histograms show that compared to DHFR(DD)-YFP or DHFR(DD)-Flt23k, stabilized DHFR(DD)-Flt23k inhibits intracellular (**a**) and extracellular (**b**) VEGF expression, as detected by ELISA. One-way ANOVA followed by Tukey's multiple comparisons test was performed to determine the significance of differences (***$p<0.001$, **$p<0.01$, *$p<0.05$). All data are presented as the mean ± SEM. mCH, mCherry; YFP, yellow fluorescent protein; TMP, trimethoprim

with 10 μM TMP: 63 ± 13 pg/μg, $p<0.05$; DHFR(DD)-Flt23k with 50 μM TMP: 45 ± 14 pg/μg, $p<0.01$; $n=8$) (Fig. 2a). Similarly, the cells transfected with pscAAV-DHFR(DD)-Flt23k also showed a significant TMP-dependent decrease in extracellular VEGF secretion (DHFR(DD)-Flt23k: 1192 ± 79 pg/mL; DHFR(DD)-Flt23k with 2 μM TMP: 828 ± 89 pg/mL; DHFR(DD)-Flt23k with 10 μM TMP: 601 ± 97 pg/mL, $p<0.01$; DHFR(DD)-Flt23k with 50 μM TMP: 507 ± 92 pg/mL, $p<0.001$; $n=7$) (Fig. 2b). Together, our in vitro data suggest that gene delivery of DHFR(DD)-Flt23k can reduce the VEGF protein level in a TMP-controlled manner.

Interestingly, we also found that cells transfected with pscAAV-DHFR(DD)-YFP (intracellular VEGF: 388 ± 33 pg/μg, $n=7$; extracellular VEGF: 1544 ± 92 pg/mL, $n=8$) showed a significant decrease in intracellular (153 ± 24 pg/μg, $p<0.001$, $n=8$) and extracellular (932 ± 113 pg/mL, $p<0.01$, $n=7$) VEGF levels when exposed to 50 μM TMP (Fig. 2a). We investigated whether the high dose of TMP inhibits VEGF expression using quantitative polymerase chain reaction (qPCR). Under hypoxic conditions, cells were exposed to TMP at a dose between 0.01 and 100 μM, and compared to no TMP, cells treated with high dose of TMP (100 μM) decreased VEGF gene expression (Fig. S1a). We then confirmed that compared to cells not treated with TMP, cells transfected with pscAAV-DHFR(DD)-YFP (fold change in *VEGFA* mRNA: 8.1 ± 0.7, $p<0.05$; $n=3$) or pscAAV-DHFR(DD)-Flt23k (fold change in *VEGFA* mRNA: 7.8 ± 0.4, $p<0.05$; $n=3$) and then exposed to 50 μM TMP also showed a decrease in VEGF gene expression (DHFR(DD)-YFP: 17.2 ± 1.9; DHFR(DD)-Flt23k: 15.0 ± 1.6; $n=3$) (Fig. S1b). Thus, our results indicate that a high dose of TMP (> 10 μM) may also influence VEGF gene expression.

Validation of transgene product regulation by the DHFR(DD)-protein-destabilizing system in rat retinas

The rat OIR model was employed to evaluate the therapeutic potential of drug-tunable Flt23k gene therapy in retinal neovascularization. We first assessed the effectiveness of scAAV2-mediated gene delivery in OIR rats. Eleven days after intravitreal injection of scAAV2-EGFP into OIR rats (postnatal day 18 [P18]), EGFP expression was evident across the whole flat-mount retina (Fig. 3a). Retinal cross-sections also showed that scAAV2 drove strong panretinal expression across all retinal layers (including the ganglion cell layer, inner nuclear layer and outer nuclear layer), as evidenced by the presence of EGFP (Fig. 3b). Given that retinal glia are a potential cellular source of VEGF, we further characterized scAAV2-mediated transgene expression in retinal glial cells using colabeling of glial fibrillary acidic protein (GFAP; a marker of glial cells). We found that scAAV2 was able to drive gene expression in GFAP-positive retinal glial cells (Fig. 3c).

To verify the hypothesis that DHFR(DD) provides control of the expressed fusion protein in vivo, P7 rat pups were intravitreally injected with scAAV2-DHFR(DD)-YFP and then received an intraperitoneal injection of 3 μg TMP on

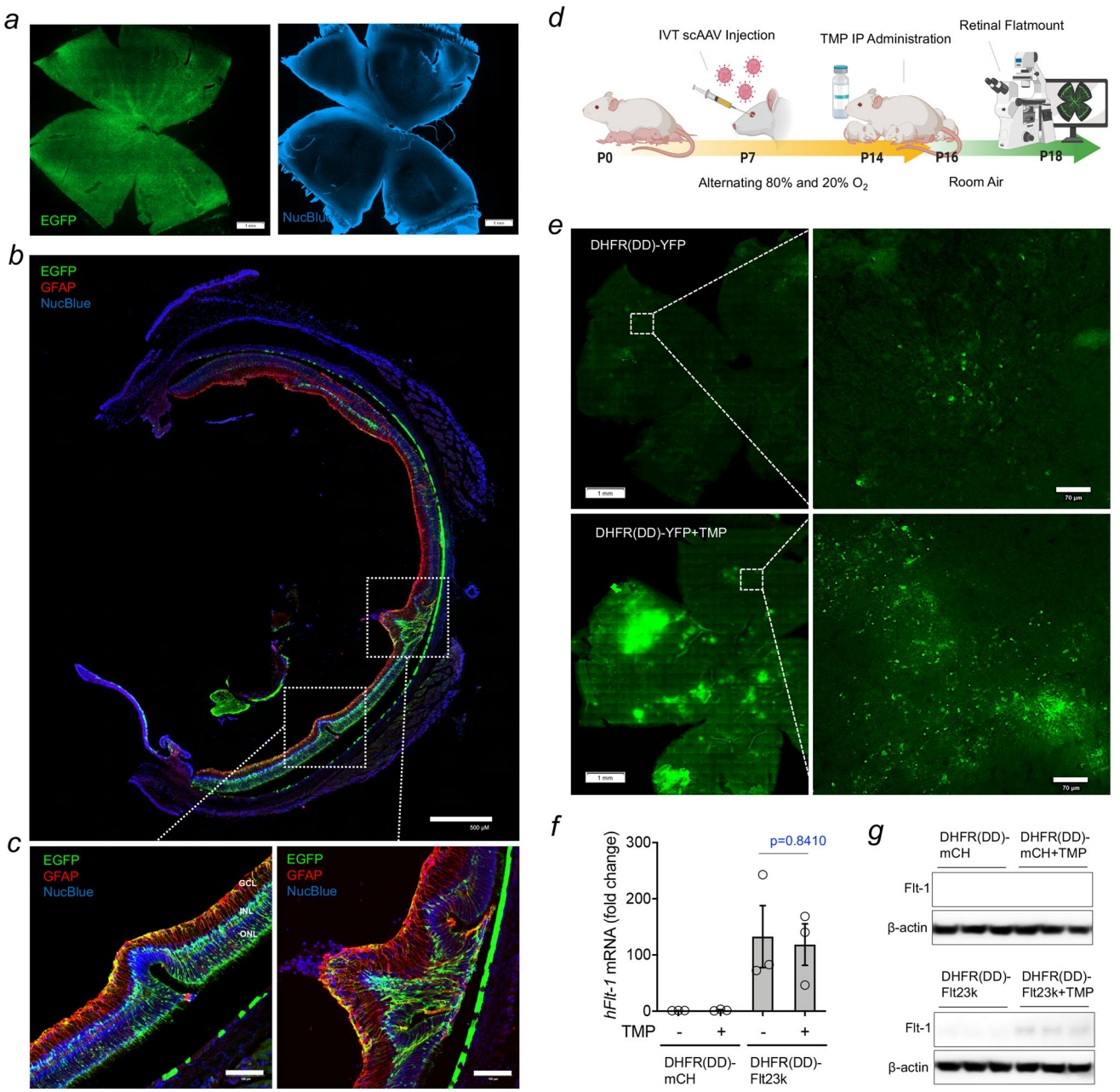

Fig. 3 scAAV2-mediated gene transduction following intravitreal injection into the retina of OIR rats. Representative images of retinal flat-mount sections (**a**) and cross-sections (**b** and **c**) from OIR rats (P18) 11 days after scAAV2-EGFP intravitreal injection. Intact retinas were confirmed with NucBlue™ (blue) staining. **a** Retinal flat mounts showing EGFP expression distribution (green). Scale bars: 1 mm. **b** Distribution and colocalization of EGFP (green) and GFAP staining (retinal glial cell marker, red) in retinal cross-sections. Scale bars: 500 µm. **c** High-magnification view of a retinal cross-section. Transduction of retinal cells is evident by the presence of EGFP-positive cells in the outer nuclear layer (arrows) and inner segments. Scale bars: 100 µm. **d** Schematic diagram of the rat OIR model protocol to illustrate the timing of viral vector injection and intraperitoneal TMP injection. **e** Retinal flat-mount section showing TMP-mediated YFP protein stabilization in an OIR rat. Scale bars: 1 mm (left panels) and 70 µm (right panels). **f** DHFR(DD)-Flt23k mRNA expression levels in retinas injected with scAAV2-DHFR(DD)-mCherry or scAAV2-DHFR(DD)-Flt23k with or without TMP, as quantified using qPCR ($n=3$). Two-tailed Student's *t*-tests were performed to evaluate differences between groups. All data are presented as the mean ± SEM. **g** Retinal DHFR(DD)-Flt23k protein levels determined using western blotting, each with three replicates. Corresponding uncropped images of western blots are shown in Figure S6. OIR, oxygen-induced retinopathy; EGFP, enhanced green fluorescent protein; GFAP, glial fibrillary acidic protein; mCH, mCherry; YFP, yellow fluorescent protein; TMP, trimethoprim; GCL, ganglion cell layer; INL, inner nuclear layer; ONL, outer nuclear layer

P14 and P16. Eyes were harvested on P18 to validate the expression of DHFR(DD)-YFP (Fig. 3d). We found that a few YFP fluorescence-positive cells were present without TMP treatment but YFP protein levels were significantly elevated after the stabilization of DHFR(DD)-YFP by systemic injection of TMP (Figs. 3e and S2). A similar pattern indicating a drug-tunable effect was shown in scAAV2-DHFR(DD)-mCherry-treated retinas of OIR rats (Fig. S3). To further verify that the drug-tunable effect of the DHFR(DD)-fusion protein is mediated through posttranslational regulation, DHFR(DD)-Flt23k mRNA and protein levels in the retinas of OIR rats were quantified using qPCR and western blotting. DHFR(DD)-Flt23k gene expression was significantly increased in retinas from scAAV2-DHFR(DD)-Flt23k-injected rats compared with those from scAAV2-DHFR(DD)-mCherry-injected rats (Fig. 3f). No statistically significant difference ($p = 0.8410$) in the DHFR(DD)-Flt23k mRNA level was found between scAAV2-DHFR(DD)-Flt23k-injected rats treated with TMP (118.5 ± 36.95-fold; $n = 3$) and those not treated with TMP (132.7 ± 55.14-fold; $n = 3$). DHFR(DD)-Flt23k proteins were detected only in retinas from scAAV2-DHFR(DD)-Flt23k/TMP-injected rats; no protein was found in retinas from scAAV2-mCherry- or scAAV2-DHFR(DD)-Flt23k/vehicle-injected rats (Fig. 3g). These results demonstrate that scAAV2 can effectively deliver DHFR(DD)-Flt23k to the retina in OIR rats and that subsequent administration of TMP is able to stabilize the expressed DHFR(DD)-Flt23k protein.

scAAV2-mediated gene delivery of DHFR(DD)-Flt23k reduces VEGF levels and attenuates retinal neovascularization in the OIR rat model

The rat OIR model was applied to evaluate the therapeutic potential of drug-tunable DHFR(DD)-Flt23k gene therapy in retinal neovascularization. P7 pups were intravitreally injected with scAAV2-mCherry, scAAV2-Flt23k, scAAV2-DHFR(DD)-mCherry or scAAV2-DHFR(DD)-Flt23k. On P14 and P16, rats received intraperitoneal injections of TMP. Eyes were then harvested on P18 to evaluate VEGF expression and pathological blood vessel formation on the surface of the retina (retinal neovascularization; Figs. 4a and S4a). Increased mRNA and protein expression of VEGF was observed in the retina of OIR rats on P18 (Fig. S4b and S4c). Compared with eyes that received scAAV2-mCherry (VEGF: 39.9 ± 4.1 pg/mL; $n = 8$), those intravitreally injected with scAAV2-Flt23k (VEGF: 28.5 ± 2.6 pg/mL, $p < 0.05$; $n = 8$) showed a significantly reduced level of VEGF in the retina (Fig. 4b). Surprisingly, we found that VEGF expression was significantly reduced in retinas from scAAV2-DHFR(DD)-Flt23k/vehicle-injected rats (VEGF: 27.3 ± 1.5 pg/mL, $p < 0.05$; $n = 8$) and scAAV2-DHFR(DD)-Flt23k/TMP-injected rats (VEGF: 22.9 ± 1.4 pg/mL, $p < 0.01$; $n = 8$) compared with those from scAAV2-DHFR(DD)-mCherry/vehicle-injected rats (VEGF: 42.3 ± 4.8 pg/mL; $n = 8$) or scAAV2-DHFR(DD)-mCherry/TMP-injected rats (VEGF: 37.8 ± 3.7 pg/mL; $n = 8$) (Fig. 4b). A further reduction in the retinal VEGF level was found in scAAV2-DHFR(DD)-Flt23k/TMP-injected rats compared to scAAV2-DHFR(DD)-Flt23k/vehicle-injected rats, but this difference did not reach statistical significance ($p = 0.0508$) (Fig. 4b). The results indicate that DHFR(DD)-Flt23k can reduce VEGF levels in the retina even without TMP administration.

We subsequently evaluated the therapeutic potential of the drug-tunable Flt23k gene delivery system in retinal neovascularization in vivo. Small tufts of vascular endothelial cells were observable at the edge of new blood vessel growth adjacent to avascular areas (Figs. 4c and S5). Compared with intravitreal injection of scAAV2-mCherry (neovascular area: $3.23 \pm 0.25\%$ [95% confidence interval (CI) 2.68–3.78]; $n = 15$), intravitreal injection of scAAV2-Flt23k significantly inhibited neovascularization (neovascular area: $1.57 \pm 0.14\%$ [95% CI 1.28–1.86], $p < 0.001$; $n = 20$) (Fig. 4d). In the drug-tunable system, a significant inhibition of retinal neovascularization was observed between scAAV2-DHFR(DD)-Flt23k-injected rats treated with TMP ($1.28 \pm 0.13\%$ [95% CI 1.02–1.55], $p < 0.05$; $n = 20$) and those not treated with TMP ($1.95 \pm 0.12\%$ [95% CI 1.69–2.20]; $n = 23$) (Fig. 4d). Similarly, there was a significant reduction in the neovascular area ($1.28 \pm 0.13\%$ [95% CI 1.02–1.55], $p < 0.001$; $n = 20$) in retinas from scAAV2-DHFR(DD)-Flt23k/TMP-injected rats compared with those from scAAV2-DHFR(DD)-mCherry/TMP-injected rats (neovascular area: $2.94 \pm 0.25\%$ [95% CI 2.40–3.48]; $n = 17$) (Fig. 4d). We also found a reduction in the retinal neovascular area in scAAV2-DHFR(DD)-Flt23k/vehicle-injected rats (neovascular area: $1.95 \pm 0.12\%$ [95% CI 1.69–2.20], $p < 0.01$; $n = 23$) compared with rats injected with scAAV2-DHFR(DD)-mCherry/vehicle (neovascular area: $2.49 \pm 0.23\%$ [95% CI 2.00–2.98]; $n = 19$) (Fig. 4d). Moreover, no significant difference in the avascular area was observed among the 6 groups (Fig. 4e). Together, our results demonstrate that gene delivery of DHFR(DD)-Flt23k by scAAV2 allows controlled suppression of retinal neovascularization in OIR rats via the administration of TMP.

Discussion

In the present study, we demonstrate that the DHFR(DD)-protein-destabilizing system may be a promising way to regulate the level of Flt23k in the retina for tailored suppression of retinal neovascularization. Our in vitro studies showed that fusion of Flt23k to the N-terminus of DHFR(DD) allowed relatively good control of Flt23k expression with

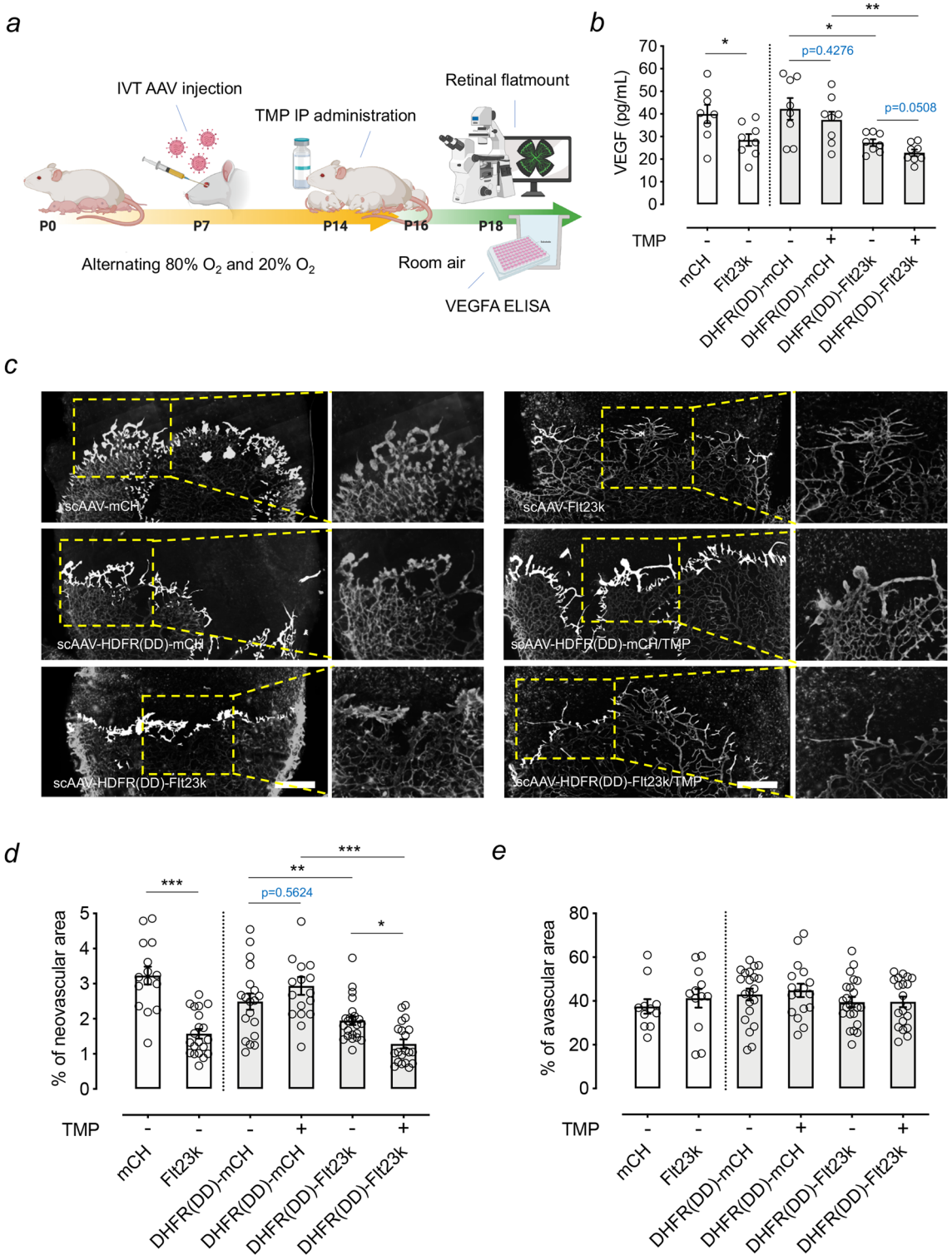

TMP. We showed that in a dose-dependent manner, TMP increased the expression of Flt23k, which was functional with the capacity to attenuate intracellular and extracellular VEGF levels in cells exposed to hypoxic conditions. Finally, intravitreal gene delivery of DHFR(DD)-Flt23k by scAAV2 and subsequent administration of TMP provided evidence for tunable attenuation of ischemia-induced retinal neovascularization in a rat model of OIR.

Rapid advances in gene therapy have brought this approach nearly to clinical use in ophthalmology. Given that the eye is a particularly favorable organ for gene delivery, ocular use is likely to be among the most successful

◂**Fig. 4** Effects of intravitreal scAAV2-DHFR(DD)-Flt23k injection on retinal neovascularization in the rat OIR model. **a** Schematic of the rat OIR model protocol to illustrate the timing of viral vector injection and intraperitoneal TMP injection. Neonatal rats were exposed to daily cycles of 80% oxygen for 21 h and room air for 3 h from P0 to P14 and received an intraperitoneal injection of 3 mg of TMP on P14 and P16. On P14, the animals were returned to room air until P18. scAAV2-mCherry, scAAV2-Flt23k, scAAV2-DHFR(DD)-mCherry, or scAAV2-DHFR(DD)-Flt23k was injected on P7. **b** Rat retinal VEGF levels quantified using ELISA (n=8 retinas from 3 littermates). One-way ANOVA followed by Tukey's multiple comparisons test was performed to determine the significance of differences (**$p<0.01$, *$p<0.05$). **c** A typical cluster of vascular structures represented as "neovasculature" on a flat-mounted retina harvested on P18 after intravitreal injections on P7 and stained with isolectin B4. Retinal neovascularization is highlighted in white, and insets show the selected areas at high magnification. Scale bars: 250 µm. Corresponding uncropped images of retinas are shown in Figure S5. **d** Retinal neovascular area quantification (n=15–23 retinas). One-way ANOVA followed by Tukey's multiple comparisons test was performed to compare groups (***$p<0.001$, **$p<0.01$, *$p<0.05$). **e** Retinal avascular area quantification (n=11–22 retinas). No significant difference was observed in the avascular area. All data are presented as the mean ± SEM. OIR, oxygen-induced retinopathy; mCH, mCherry; TMP, trimethoprim

applications of this technique. We provided proof-of-principle evidence that intravitreal injection of scAAV2 under a ubiquitous cytomegalovirus (CMV) promoter in OIR rats resulted in efficient and high-level transgene expression within a time frame relevant to the treatment of retinal neovascularization. scAAV2 has been shown to exhibit better transduction efficiency and faster initiation of gene expression in the retina than conventional single-stranded AAVs [13, 14]. However, the ubiquitous CMV promoter cannot be used to express anti-VEGF therapeutic genes in specific cell types (i.e., Müller glial cells and photoreceptors) that are the primary source of VEGF production in proliferative retinopathies. As such, it will be important to develop a better delivery system with either a cell-specific promoter or an AAV variant that targets desired cell types. Such refinements will lead to more effective therapies while reducing the potential for adverse effects.

In this study, we show that using scAAV2 to deliver Flt23k can modify VEGF levels and reduce retinal neovascularization in OIR rats. A similar therapeutic effect was also observed with AAV-mediated gene delivery of Flt23k in a murine model of choroidal neovascularization [11]. However, high-level expression of an anti-VEGF protein such as Flt23k in the retina may have unwanted consequences. Strategies are needed to regulate transgene expression through the incorporation of trigger elements into the expression cassette, which are then modulated by an exogenous drug [15] or endogenous molecules generated as part of the disease process [16]. Different from those approaches, a protein-destabilizing system based on *E. coli* DHFR(DD) was used here. In this system, the engineered DHFR(DD) is rapidly degraded along with any attached protein. A small molecule pharmacological chaperone (protein stabilizer) such as TMP, a common antibiotic, allows newly synthesized DDs to be folded and stabilized at higher steady-state levels within cells, thus protecting the attached therapeutic protein from degradation [17]. An appealing aspect of this strategy to stabilize therapeutic proteins is that TMP, which is safe and able to cross the blood-retina barrier, can be administered orally at a chosen time, such as during an exacerbation of retinal angiogenesis [9]. Oral or topical administration of TMP reliably prevents proteasomal destruction of DHFR (DD)-fused proteins (delivered via an AAV) in the rodent retina without impacts on retinal function or structure [9, 11]. Thus, TMP-mediated tunable gene therapy could meet the clinical requirement for a tailored and sustained therapeutic intervention to treat retinal neovascularization.

Although promising in several regards, the DHFR(DD) destabilizing system requires further refinement. Specifically, we observed that low protein levels of DHFR(DD)-Flt23k were present in transfected cells not treated with TMP, suggesting that not all DHFR(DD)-fusion proteins were degraded. Indeed, a significant reduction in the cytosolic VEGF level was seen in DHFR(DD)-Flt23k-transfected cells and the retina of scAAV2-DHFR(DD)-Flt23k-injected eyes without the addition of TMP. Additionally, Flt23k is a recombinant construct consisting of domain 2/3 of the VEGFR1 receptor coupled with a C-terminal ER-retention signal sequence (KDEL) [10]. The ER-retention signal sequence allows newly formed fusion proteins to be retained in the ER [18], thus delaying their degradation and leading to VEGF binding. However, newly formed fusion proteins may generate a pull effect between the ER-retention signal and the protein-destabilizing signal of DHFR(DD)-Flt23k, which may result in a delay in protein degradation, thereby increasing the amount of undegraded protein in the cytosol. The undegraded or intermediate DHFR(DD)-Flt23k protein can potentially neutralize cytosolic VEGF and modulate the angiogenic response even without TMP stabilization. This might account for our observation that retinal neovascularization was reduced in scAAV2-DHFR(DD)-Flt23k-treated rats compared to those that received scAAV2-DHFR(DD)-mCherry. As OIR is a relatively acute model of retinal neovascularization with a low level of VEGF upregulation, a mild VEGF suppression can impact neovascularization. Thus, rats receiving scAAV2-DHFR(DD)-Flt23k express low levels of undegraded or intermediate DHFR(DD)-Flt23k protein, which could neutralize retinal VEGF over time. A higher protein level of stabilized DHFR(DD)-Flt23k was observed upon TMP injection on P14 and P16 and led to more effective neutralization and thus a greater suppressive effect on retinal neovascularization. Therefore, our drug-tunable Flt23k gene therapy might be improved by removing the ER-retention signal sequence and adjusting the viral

dose to reduce basal VEGF inhibition. Further studies in a clinically relevant model of chronic retinal neovascularization will further inform differences in the benefits of this tunable system.

A limitation of our work was that the safety of the drug-tunable Flt23k gene therapy in the retina was not evaluated in this proof-of-concept study. However, two recent studies have reported the safety profile of retinal Flt23k gene therapy and systemic TMP administration in mice. Zhang et al. reported that subretinal AAV-mediated gene delivery of Flt23k had no impact on retinal function or morphology for up to 6 months [11]. Datta et al. showed that there was no impact on the visual function or structure of the mouse retina after 3 months of TMP treatment [9]. Although these two studies have indicated that these strategies are safe in the retina, it will be important to assess the safety of both AAV-mediated Flt23k gene delivery and TMP administration before current research can be clinically translated. Another limitation of the present study was that the treatment was evaluated with a single dose of TMP (10 mg/kg) over a relatively short period of time in OIR rats. The TMP dose used in this study was based on published reports [8, 9] and is within the recommended dose for humans (10–15 mg/kg) [19]. As indicated by other reports and our in vitro data, the dose of TMP impacts the expression of the stabilized DHFR(DD)-Flt23k protein. Therefore, the dose and frequency of TMP administration will need to be further optimized to match a drug-tunable Flt23k gene therapy system to the protracted time course of clinical disease processes.

Consistent with previous studies, this study showed that protein expression was dependent on the TMP dose. Although maximizing the TMP dose to achieve the optimal therapeutic effect is critical, the systemic administration of high-dose TMP may also have deleterious effects. Indeed, our in vitro study showed that a high dose of TMP impairs VEGF mRNA expression (Fig. S1). It has been reported that high doses of TMP can induce cell toxicity [20], thus this insult may result in modifying VEGF mRNA expression. Therefore, administration of high-dose TMP together with DHFR(DD)-Flt23k gene delivery may act synergistically to suppress VEGF at both the transcriptional level and the posttranslational level. In addition, prolonged oral TMP administration has been shown to disrupt the gut microbiome, which can impact the central nervous system [21] and in turn modify the progression of ocular diseases [22]. Thus, topical administration of TMP via eye drops may be a safer alternative. One study of the rodent retina demonstrated that topical administration of TMP could reliably and locally stabilize the expression of proteins fused to DHFR(DD) (delivered via an AAV) [9]. Moreover, to further mitigate systemic adverse events, a TMP-based nonantibiotic small molecule has been developed to control DHFR(DD)-fused proteins [23]. Therefore, a combination of nonantibiotic eye drops and tunable Flt23k gene therapy would be a safe and attractive approach for the treatment of retinal neovascularization.

In summary, our data suggest that the DHFR(DD)-protein-destabilizing system is a promising way to regulate the level of Flt23k in the retina and provides the potential to tailor suppression of retinal neovascularization. Although further investigations are required to assess long-term safety and efficacy in clinically relevant models, we believe that this comprehensive strategy has the potential as a treatment strategy for retinal neovascularization and avoids the need for repeated intravitreal injections.

Materials and methods

The sources of the materials and equipment used in this study are listed in Table S1.

Cell culture

HEK293A (catalog no. R70507; Life Technologies Australia, Mulgrave, VIC, Australia) and HEK293D (a gift from Dr. Ian Alexander at the Children's Medical Research Institute, University of Sydney, Australia) cells were cultured in Dulbecco's modified Eagle's medium (DMEM; catalog no. 11965092; Life Technologies Australia) supplemented with 10% fetal bovine serum (catalog no. F9423; Sigma-Aldrich, St. Louis, MO, USA), 50 U/mL penicillin–streptomycin (catalog no. 15070-063; Life Technologies Australia) and 2 mM glutamine (catalog no. 2503008; Life Technologies Australia). Cell lines were confirmed to be free of mycoplasma using the MycoAlert™ Mycoplasma Detection Kit (catalog no. LT07; Lonza, Walkersville, MD, USA) and cultured in a humidified 5% CO_2 atmosphere at 37 °C.

Transfection

Plasmid transfection was performed with Lipofectamine 2000 (catalog no. 11668019; Life Technologies Australia). In brief, HEK293A cells were plated in a 6-well plate on day 0 ($2.5x10^5$/well) and transfected with 750 ng of plasmid DNA using the protocol provided in the kit. After 24 h of incubation, the transfection medium was replaced with fresh medium and treated with TMP (0, 2, 10, or 50 μM; catalog no. T7883; Sigma-Aldrich). Thereafter, cells were either exposed to hypoxia (GENbag anaer hypoxia bag, catalog no. 45534; bioMeriux, Marcy-l'Étoile, France) or kept in normoxia for 24 h. Cell lysates and conditioned medium were then harvested for ELISA and qPCR.

AAV construction and virus production

EGFP, mCherry, Flt23k, DHFR(DD)-YFP, DHFR(DD)-mCherry, Flt23k-DHFR(DD) and DHFR(DD)-Flt23k complementary DNA (cDNA) sequences surrounded by AgeI/NotI cleavage sites were obtained by gene synthesis (GenScript, Piscataway, NJ, USA) and subcloned into the pHpa-trs-SK-EGFP plasmid (a gift from Dr. Douglas M. McCarty at the Center for Gene Therapy, Nationwide Children's Hospital, USA) by replacing the EGFP sequence. The Flt23k DNA sequence was kindly provided by Dr. Balamurali K Ambati at the Moran Eye Center (University of Utah, USA). The DHFR(DD) DNA sequence was based on pBMN-DHFR(DD)-YFP (a gift from Dr. Thomas Wandless at the Stanford University, USA; Addgene plasmid #29325). Recombinant scAAV2s were packaged as previously described [24]. Briefly, the scAAV2s were prepared by transfecting HEK293D cells with the targeted plasmids (pscAAV-mCherry, pscAAV-Flt23k, pscAAV-DHFR(DD)-YFP, pscAAV-DHFR(DD)-mCherry, pscAAV-DHFR(DD)-Flt23k or pHpa-trs-SK-EGFP), a helper plasmid (pXX6, kindly provided by the UNC Vector Core Facility, USA) and an AAV2 capsid plasmid (pXX2, kindly provided by the UNC Vector Core Facility, USA) using the calcium phosphate method. Viral vectors were purified using the AAVpro Purification Kit (catalog no. 6666; Clontech Laboratories, Mountain View, CA, USA), and titers were quantified by qPCR.

Western blot analysis

Cells or retinas were collected in 150 µL of Pierce RIPA buffer (catalog no. 89900; Life Technologies Australia) with a protease inhibitor cocktail (catalog no. 14692300; Roche Diagnostics, Basilea, Swiss). The lysates were homogenized using a sonicator for 5–10 s and then centrifuged at full speed for 15 min at 4 °C. The supernatants were collected and quantified using a Pierce™ BCA assay kit (catalog no. 23227; Life Technologies Australia). Proteins were denatured at 85 °C for 10 min, followed by separation on NuPAGE™ Novex™ 4–12% Bis–Tris Protein Gels (catalog no. NP0321BOX; Life Technologies Australia) using gel electrophoresis and transfer to polyvinylidene fluoride membranes (catalog no. IPVH00010; Immobilon-P; Merck Millipore, Burlington, MA, USA) using the XCell II™ Blot Module (Life Technologies Australia) at 30 volts for 1 h. The membranes were then blocked with 5% skim milk in TBS-T (10 mM Tris, 150 mM NaCl, and 0.05% Tween-20) at room temperature for 1 h and incubated with a mouse anti-VEGFR1 antibody (Flt-1/EWC) (1:500 dilution; catalog no. ab9540; Abcam, Cambridge, UK) overnight at 4 °C or with a mouse anti-GAPDH antibody (clone 6C5, 1:500 dilution; catalog no. MAB374; Merck Millipore) or mouse anti-Actin antibody (clone C4, 1:5000 dilution; catalog no. MAB1501; Merck Millipore) at room temperature for 1 h. The membranes were washed and further incubated with a goat anti-mouse IgG HRP-conjugated secondary antibody (1:4000 dilution; catalog no. 12-349; Merck Millipore) at room temperature for 1 h. The membranes were then developed using the Amersham ECL Prime Western Blotting Detection Kit (catalog no. RPN2235; GE Healthcare Australia, Parramatta, NSW, Australia).

ELISA

The VEGF protein level was detected in HEK293A cell lysates, conditioned media and rat retinal tissue lysates using ELISA. For cell and tissue lysates, samples were prepared in Pierce RIPA buffer. Lysates and conditioned media were analyzed using human or rat VEGF ELISA kits (catalog no. DY293B and RRV00; R&D Systems, Inc., Minneapolis, MN, USA) per the manufacturer's instructions, and results were read at a 450-nm wavelength using a CLARIOstar microplate reader (BMG LABTECH, Ortenberg, Germany).

qPCR

Total RNA was extracted and purified from cells or retinas using TRIzol Reagent (catalog no. 15596026; Life Technologies Australia) according to the manufacturer's instructions. cDNA synthesis from total RNA was achieved using a high-capacity RT kit (catalog no. 4368814; Life Technologies Australia). Two nanograms of cDNA were used for real-time PCR using an ABI QuantStudio3 device (Applied Biosystems, Foster City, CA, USA) and TaqMan Fast Master mix (catalog no. 4444557; Life Technologies Australia) with the TaqMan assay probes for *VEGFA* (Hs00900054_m1). Human *HPRT1* (Hs99999909_m1) was used as the reference gene. Transcript levels were calculated using the ΔΔCt method, as previously described by Livak [25].

Animals

Female Sprague–Dawley rats were supplied by the Cambridge Farm Facility of the University of Tasmania and housed in standard cages with free access to food and water in a temperature-controlled environment under a 12-h light (50 lx illumination)/12-h dark (< 10 lx illumination) cycle to minimize possible light-induced eye damage. All animal experiments described adhered to the guidelines of the Association for Research in Vision and Ophthalmology Statement for the Use of Animals in Ophthalmic and Vision Research and were approved by the Animal Ethics Committee of the University of Tasmania, Australia (ethics approval number A0017598).

Rat model of OIR and vessel quantification

We employed a modified rat OIR protocol based on a previous study [26]. Briefly, newborn Sprague–Dawley rats and their nursing mothers were housed in a commercially available chamber (A-Chamber; BioSpherix, Parish, NY, USA) within 12 h of birth (P0) and exposed to daily cycles of 80% O_2 for 21 h and room air for 3 h from P0 to P14. The pups were then returned to room air until P18. An oxygen controller (ProOx 110; BioSpherix) was used to monitor and control the oxygen level in the humidified chamber. The rats were sacrificed on P18, and their retinas were dissected and stained with 5 g/mL Alexa Fluor™ 488-conjugated isolectin B4 (isolectin GS-IB4 from *Griffonia simplicifolia*; catalog no. I21411; Life Technologies Australia). The sizes of the neovascularization and vaso-obliteration areas in the rat retinas were quantified with Adobe Photoshop (CC 2017.1.1) by two blinded assessors (JC and GSL). If the isolectin GS-IB4-labeled retinal vascular area was < 20% of the total retinal area, the sample was excluded from the study.

Intravitreal injection

Intravitreal injections of AAVs were performed under a surgical microscope. In brief, after making a guide track through the conjunctiva and sclera at the superior temporal hemisphere behind the limbus using a 30-gauge needle, a hand-pulled glass micropipette connected to a 10-µL Hamilton syringe (Bio-Strategy, Broadmeadows, VIC, Australia) was inserted into the vitreal cavity. A total of 1 µL of AAVs (2–2.5 × 10^9 viral genomes) was injected into an eye of OIR rats on P7, and an equal amount of saline was injected into the contralateral eye of the same animal. A total of 192 neonatal rats (from 20 litters) were used in our in vivo study. Animals were randomly allocated into the following groups: scAAV2-EGFP ($n = 5$), scAAV2-mCherry ($n = 29$), scAAV2-Flt23k ($n = 30$), scAAV2-DHFR(DD)-YFP ($n = 10$), scAAV2-DHFR(DD)-mCherry ($n = 52$), and scAAV2-DHFR(DD)-Flt23k ($n = 66$). Any issues arising from the injection, including large backflow upon removal of the needle and the presence of hemorrhaging anywhere on the eye, resulted in exclusion from the study.

TMP administration

OIR rats were intraperitoneally injected with a TMP lactate salt (catalog no. T0667; Sigma-Aldrich) or vehicle on P14 and P16. TMP was freshly dissolved in nanopure water and diluted to a concentration of 30 mg/mL. Rats were given 100 µL of this solution, which equates to 3 mg of TMP/rat/dose.

Immunofluorescence analysis

Rat pups were euthanized on P18. Eyeballs were removed and fixed in a 4% formaldehyde solution in PBS for 1 h at room temperature. The cornea and lens were removed, and the globes were incubated with 18% sucrose until the eyeball sank to the bottom of the container at room temperature. The eyes were then placed in 30% sucrose overnight. Samples were embedded in optimal cutting temperature compound (catalog no. IA018; ProSciTech, Kirwan, QLD, Australia) and stored at − 80 °C. Serial cryosections (20-µm thickness) were obtained and stored at − 20 °C. The sections were rinsed in three washes of PBS and then underwent immunofluorescence labeling with NucBlue™ Live Cell Stain ReadyProbes Reagent (catalog no. R3760S; Life Technologies Australia) for 20 min and an anti-GFAP antibody (1:500 dilution; catalog no. G3893; Merck Millipore) for 1 h. The sections were washed and mounted with Dako fluorescent mounting medium (catalog no. s3020; DAKO, Carpinteria, CA, USA). Images were digitized using a fluorescence microscope (Zeiss Axio Imager Microscope; Carl-Zeiss-Strasse, Oberkochen, Germany) equipped with a charge-coupled digital camera (Axiocam MRm, Zeiss) and image acquisition software (ZEN2, Zeiss). The entire retina was photographed using appropriate filters to capture the fluorescence emission spectra of mCherry (610 nm), EGFP/isolectin B4-FITC (509 nm), and NucBlue (460 nm), and separate images were merged to form a complete image of the retinal section. The fluorescence of the EGFP-positive area in the total retina was quantified with ImageJ.

Statistical analysis

Statistical analysis was performed using GraphPad Prism 7 for all experimental data. Measurement data are presented as the mean ± standard error of the mean (SEM). Comparisons among multiple groups were analyzed by two-tailed Student's *t*-tests, one-way or two-way ANOVA followed by Tukey's multiple comparisons. Values were determined to be significant when the p value was less than 0.05.

Acknowledgements The authors thank UTAS CFF animal technicians, Karen Shiels, Keri Smith, Heather Howard, Lisa Harding and Danielle Eastley, for their assistance with rat chamber operation. This work was supported by grants from the National Health and Medical Research Council of Australia (NHMRC; 1061912, 1185600, 1108311 and 1161583), the Ophthalmic Research Institute of Australia, the National Natural Science Foundation of China (8197030485) and the Rebecca L Cooper Medical Research Foundation. A.W.H. received an NHMRC Practitioner Fellowship (1103329). L.L. was supported by the Department of Science and Higher Education of Ministry of National Defense, Republic of Poland ("Kościuszko" k/10/8047/DNiSW/T-WIHE/3) and the National Science Centre, Republic of Poland (UMO-2017/25/B/NZ1/02790). The Centre for Eye Research

Australia receives Operational Infrastructure Support from the Victorian Government.

Author contributions Conceptualization—J.C., G-S.L. Methodology—J.C., F-L.L., J.Y.K.L., G-S.L. Formal Analysis—J.C., F-L.L., G-S.L. Investigation—J.C., F-L.L., J.Y.K.L., L.T., Y-F.C., J-H.W., F.L., V.H.Y.W. Resources—G.J.D., H.-H.S., B.V.B., L.L., A.W.H., J.Z., G-S.L. Data Curation—J.C., G-S.L. Writing (Original Draft)—J.C., G-S.L. Writing (Review & Editing)—J.Y.K.L., J-H.W., F-L.L., L.L., G.J.D., V.H.Y.W., B.V.B., J.Z. Visualization—J.C., G-S.L. Supervision—J.Z., G.S.L. Project Administration—J.C., G-S.L. Funding Acquisition—J.Z., G-S.L.

Data availability All datasets generated for this study are included in the article/supplementary materials.

Compliance with ethical standards

Competing interests The authors have declared that no competing interest exists.

References

1. Sun Y, Smith LEH (2018) Retinal vasculature in development and diseases. Annu Rev Vis Sci 4:101–122
2. Wells JA, Glassman AR, Ayala AR, Jampol LM, Aiello LP, Antoszyk AN, Arnold-Bush B, Baker CW, Bressler NM, Browning DJ, Elman MJ, Ferris FL, Friedman SM, Melia M, Pieramici DJ, Sun JK, Beck RW (2015) Aflibercept, bevacizumab, or ranibizumab for diabetic macular edema. N Engl J Med 372(13):1193–1203
3. Mehta H, Tufail A, Daien V, Lee AY, Nguyen V, Ozturk M, Barthelmes D, Gillies MC (2018) Real-world outcomes in patients with neovascular age-related macular degeneration treated with intravitreal vascular endothelial growth factor inhibitors. Prog Retin Eye Res 65:127–146. https://doi.org/10.1016/j.preteyeres.2017.12.002
4. Avery RL, Gordon GM (2016) Systemic safety of prolonged monthly anti-vascular endothelial growth factor therapy for diabetic macular edema: a systematic review and meta-analysis. JAMA Ophthalmol 134(1):21–29. https://doi.org/10.1001/jamaophthalmol.2015.4070
5. Rakoczy EP, Lai CM, Magno AL, Wikstrom ME, French MA, Pierce CM, Schwartz SD, Blumenkranz MS, Chalberg TW, Degli-Esposti MA, Constable IJ (2015) Gene therapy with recombinant adeno-associated vectors for neovascular age-related macular degeneration: 1 year follow-up of a phase 1 randomised clinical trial. Lancet 386(10011):2395–2403. https://doi.org/10.1016/s0140-6736(15)00345-1
6. Heier JS, Kherani S, Desai S, Dugel P, Kaushal S, Cheng SH, Delacono C, Purvis A, Richards S, Le-Halpere A, Connelly J, Wadsworth SC, Varona R, Buggage R, Scaria A, Campochiaro PA (2017) Intravitreous injection of AAV2-sFLT01 in patients with advanced neovascular age-related macular degeneration: a phase 1, open-label trial. Lancet 390(10089):50–61. https://doi.org/10.1016/s0140-6736(17)30979-0
7. Luo L, Zhang X, Hirano Y, Tyagi P, Barabás P, Uehara H, Miya TR, Singh N, Archer B, Qazi Y, Jackman K, Das SK, Olsen T, Chennamaneni SR, Stagg BC, Ahmed F, Emerson L, Zygmunt K, Whitaker R, Mamalis C, Huang W, Gao G, Srinivas SP, Krizaj D, Baffi J, Ambati J, Kompella UB, Ambati BK (2013) Targeted intraceptor nanoparticle therapy reduces angiogenesis and fibrosis in primate and murine macular degeneration. ACS Nano 7(4):3264–3275. https://doi.org/10.1021/nn305958y
8. Santiago CP, Keuthan CJ, Boye SL, Boye SE, Imam AA, Ash JD (2018) A drug-tunable gene therapy for broad-spectrum protection against retinal degeneration. Mol Ther 26(10):2407–2417
9. Datta S, Renwick M, Chau VQ, Zhang F, Nettesheim ER, Lipinski DM, Hulleman JD (2018) A destabilizing domain allows for fast, noninvasive, conditional control of protein abundance in the mouse eye—implications for ocular gene therapy. Investig Ophthalmol Vis Sci 59(12):4909–4920
10. Singh N, Amin S, Richter E, Rashid S, Scoglietti V, Jani PD, Wang J, Kaur R, Ambati J, Dong Z, Ambati BK (2005) Flt-1 intraceptors inhibit hypoxia-induced VEGF expression in vitro and corneal neovascularization in vivo. Investig Ophthalmol Vis Sci 46(5):1647–1652. https://doi.org/10.1167/iovs.04-1172
11. Zhang X, Das SK, Passi SF, Uehara H, Bohner A, Chen M, Tiem M, Archer B, Ambati BK (2015) AAV2 delivery of Flt23k intraceptors inhibits murine choroidal neovascularization. Mol Ther 23(2):226–234
12. Egeler EL, Urner LM, Rakhit R, Liu CW, Wandless TJ (2011) Ligand-switchable substrates for a ubiquitin-proteasome system. J Biol Chem 286(36):31328–31336. https://doi.org/10.1074/jbc.M111.264101
13. Yokoi K, Kachi S, Zhang HS, Gregory PD, Spratt SK, Samulski RJ, Campochiaro PA (2007) Ocular gene transfer with self-complementary AAV vectors. Investig Ophthalmol Vis Sci 48(7):3324–3328. https://doi.org/10.1167/iovs.06-1306
14. McCarty DM (2008) Self-complementary AAV vectors; advances and applications. Mol Ther 16(10):1648–1656. https://doi.org/10.1038/mt.2008.171
15. St-Onge L, Furth PA, Gruss P (1996) Temporal control of the Cre recombinase in transgenic mice by a tetracycline responsive promoter. Nucleic Acids Res 24(19):3875–3877
16. Prentice HM, Biswal MR, Dorey CK, Blanks JC (2011) Hypoxia-regulated retinal glial cell-specific promoter for potential gene therapy in disease. Investig Ophthalmol Vis Sci 52(12):8562–8570
17. Iwamoto M, Bjorklund T, Lundberg C, Kirik D, Wandless TJ (2010) A general chemical method to regulate protein stability in the mammalian central nervous system. Chem Biol 17(9):981–988
18. Munro S, Pelham HR (1987) A C-terminal signal prevents secretion of luminal ER proteins. Cell 48(5):899–907. https://doi.org/10.1016/0092-8674(87)90086-9
19. Sulfamethoxazole/Trimethoprim Dosage (2019) https://www.drugs.com/dosage/sulfamethoxazole-trimethoprim.html
20. Güzel Bayülken D, Bostancıoğlu RB, Koparal AT, Ayaz Tüylü B, Dağ A, Benkli K (2018) Assessment of in vitro cytotoxic and genotoxic activities of some trimethoprim conjugates. Cytotechnology 70(3):1051–1059. https://doi.org/10.1007/s10616-018-0187-7
21. Carabotti M, Scirocco A, Maselli MA, Severi C (2015) The gut-brain axis: interactions between enteric microbiota, central and enteric nervous systems. Ann Gastroenterol 28(2):203–209
22. Rowan S, Jiang S, Korem T, Szymanski J, Chang ML, Szelog J, Cassalman C, Dasuri K, McGuire C, Nagai R, Du XL, Brownlee M, Rabbani N, Thornalley PJ, Baleja JD, Deik AA, Pierce KA, Scott JM, Clish CB, Smith DE, Weinberger A, Avnit-Sagi T, Lotan-Pompan M, Segal E, Taylor A (2017) Involvement of a gut-retina axis in protection against dietary glycemia-induced age-related macular degeneration. Proc Natl Acad Sci USA 114(22):E4472–e4481. https://doi.org/10.1073/pnas.1702302114
23. Peng H, Chau VQ, Phetsang W, Sebastian RM, Stone MRL, Datta S, Renwick M, Tamer YT, Toprak E, Koh AY, Blaskovich MAT, Hulleman JD (2019) Non-antibiotic small-molecule regulation of DHFR-based destabilizing domains in vivo. Mol Ther Methods Clin Dev 15:27–39

24. Xiao X, Li J, Samulski RJ (1998) Production of high-titer recombinant adeno-associated virus vectors in the absence of helper adenovirus. J Virol 72(3):2224–2232
25. Livak KJ, Schmittgen TD (2001) Analysis of relative gene expression data using real-time quantitative PCR and the 2(-Delta Delta C(T)) Method. Methods 25(4):402–408. https://doi.org/10.1006/meth.2001.1262
26. Penn JS, Tolman BL, Henry MM (1994) Oxygen-induced retinopathy in the rat: relationship of retinal nonperfusion to subsequent neovascularization. Invest Ophthalmol Vis Sci 35(9):3429–3435